Thermodynamically consistent data-driven computational mechanics

David González, Francisco Chinesta, Elías Cueto

David González · Francisco Chinesta · Elías Cueto

Thermodynamically consistent data-driven computational mechanics

Abstract In the paradigm of data-intensive science, automated, unsupervised discovering of governing equations for a given physical phenomenon has attracted a lot of attention in several branches of applied sciences. In this work, we propose a method able to avoid the identification of the constitutive equations of complex systems and rather work in a purely numerical manner by employing experimental data. In sharp contrast to most existing techniques, this method does not rely on the assumption on any particular form for the model (other than some fundamental restrictions placed by classical physics such as the second law of thermodynamics, for instance) nor forces the algorithm to find among a predefined set of operators those whose predictions fit best to the available data. Instead, the method is able to identify both the Hamiltonian (conservative) and dissipative parts of the dynamics while satisfying fundamental laws such as energy conservation or positive production of entropy, for instance. The proposed method is tested against some examples of discrete as well as continuum mechanics, whose accurate results demonstrate the validity of the proposed approach.

Keywords Data-driven computational mechanics · GENERIC · Governing equations

1 Introduction

Scientific experiments in large infrastructures are able to produce petabytes of raw data per day. With the irruption of the Internet of Things and the industry 4.0 paradigm, modern factories are also producing breathtaking amounts of data which should be stored, curated and processed so as to identify tendencies and analyze hidden correlations, patterns and, eventually, make decisions in real time. Therefore, being able to predict equations governing physical phenomena from experimental data has utmost importance. A growing interest has arose in the last years in this direction [1–5].

There are, however, physical laws of different *epistemic* nature. One cannot attribute the same importance to the second law of thermodynamics than to the response model of a new material, for instance. Often, these last equations are referred to as *constitutive* equations and have a phenomenological character. Consequently,

Communicated by Francesco dell'Isola.

D. González · E. Cueto (✉)
Aragon Institute of Engineering Research, Universidad de Zaragoza, Zaragoza, Spain
E-mail: ecueto@unizar.es

D. González
E-mail: gonzal@unizar.es

F. Chinesta
ESI Chair and PIMM Lab, ENSAM ParisTech, Paris, France
E-mail: Francisco.Chinesta@ensam.eu

the process of distilling physical laws from data in an automated way involves the task of finding *relevant* invariant structures among them—thus satisfying fundamental conservation equations—but also to be able to identify constitutive equations for the different components of the system under scrutiny.

Under non-equilibrium situations, the problem becomes even harder. An algorithm able to identify the dynamic structure of the system should be able to identify not only the conserved magnitudes (i.e., to find out its Hamiltonian structure), but also its dissipative nature. Many recent attempts in this sense begin by assuming that the (possibly nonlinear) dynamics of the system is of the form

$$\dot{z_t} = \frac{d}{dt} z(t) = \boldsymbol{f}(z(t)), \tag{1}$$

where z refers to the pertinent set of state variables, needed for an adequate description of the system. Most existing techniques are designed to search among a set of predefined operators (polynomial terms, sinus, cosinus, etc.) those that compone the operator that best fits the experimental results [6,7]. Other techniques, such as [8], progressively add terms, somehow resembling a Taylor series, until an adequate degree of accuracy is reached. More recently, the possibility of operating without any constitutive equation has also been explored [9,10]. In this last work, a set of experimental results substitute constitutive equations by developing a method that operates by finding the experimental result closest to guaranteeing equilibrium.

None of the aforementioned techniques, however, impose *a priori* any fundamental law whose satisfaction is mandatory. Thus, fundamental conservation laws will be satisfied depending on the degree of accuracy of the resulting approximation found by the different algorithms, the noise level in the data, etc. Furthermore, the set of relevant variables z—whose precise meaning will be clear hereafter—could be a priori unknown, or maybe non-relevant variables could have been stored during the experimental campaign. Detecting redundant variables is also an important issue.

In this paper, a method is proposed that guarantees the satisfaction of basic principles. Notably, conservation of energy and positive production of entropy are enforced by construction. This is possible by resorting to the so-called GENERIC structure of the problem [11]. The GENERIC paradigm generalizes the Hamiltonian structure of classical mechanics by including the dissipative properties of the problem and seems therefore to be the adequate starting point for this project. In Sect. 2, we review the basics of this paradigm. Then, in Sect. 3 we introduce a strategy for the identification of the GENERIC constituent blocks from experimental data. In Sect. 4, we propose three different examples of the performance of the method that reveals the accuracy of the proposed methodology. Finally, the paper is completed with the discussion of the results.

2 The GENERIC formalism

Under the framework of non-equilibrium thermodynamics, the GENERIC ("General Equation for Non-Equilibrium Reversible-Irreversible Coupling") formalism establishes a completely general equation of the dynamics of a system under reversible and irreversible conditions, as dictated by the evolution of energy and entropy, respectively [11,12]. GENERIC allows for a proper description of the thermodynamical structure of problems within solid and fluid mechanics, thermokinetic effects, chemical reactions or relativistic physics, among other fields in which it has been successfully applied [13]. Models constructed upon the GENERIC formalism are guaranteed to posses a sound thermodynamic structure (they preserve the symmetries of the system and therefore guarantee the subsequent conservation/dissipation laws of energy and entropy, respectively, by Noether's theorem), and therefore, it seems to be an appealing choice to start with. In addition, GENERIC paves the way to the development of numerical integration algorithms that can be seen as discrete GENERIC instances and therefore share these interesting properties [14,15].

In general, the type of systems we are considering in this work is those that can be described by the laws of classical mechanics. Under this framework, let us consider a closed, isolated system whose evolution is to be described during the time interval $\mathcal{I} = (0, T]$. The state space of the system will be described by judiciously chosen variables in a space $\mathcal{S}$. The term "judiciously chosen" will be clear hereafter. Therefore, the system will be described at time $t \in \mathcal{I}$ by a function $z_t = z(t) : \mathcal{I} \to \mathcal{S}$, $z \in \mathcal{C}^1(0, T]$.

The GENERIC structure of the evolution equations for such a system takes the form

$$\dot{z}_t = \boldsymbol{L}(z_t)\nabla E(z_t) + \boldsymbol{M}(z_t)\nabla S(z_t), \quad z(0) = z_0. \tag{2}$$

$\boldsymbol{L}$ is the so-called Poisson matrix and will be responsible for the reversible (Hamiltonian) part of the evolution of the system. E represents the energy of the system, as a function of its particular state at time t, z_t. In turn,

$\boldsymbol{M}$ represents the friction matrix, responsible for the irreversible part of the evolution of the system. Finally, S represents the entropy of the system for the particular choice of variables z. It is important to note that the actual choice of z variables is irrelevant in the sense that any other complete set of variables (possibly including a different number of them) $z' = f(z)$ will produce a valid GENERIC structure of the problem, although probably much more complex.

Equation (2) is supplemented with the complementary degeneracy conditions, i.e.,

$$\boldsymbol{L}(z) \cdot \nabla S(z) = \boldsymbol{0}, \tag{3a}$$

$$\boldsymbol{M}(z) \cdot \nabla E(z) = \boldsymbol{0}. \tag{3b}$$

By choosing $\boldsymbol{L}$ skew symmetric and $\boldsymbol{M}$ symmetric, positive semi-definite, one ensures that

$$\dot{E}(z) = \nabla E(z) \cdot \dot{z} = \nabla E(z) \cdot \boldsymbol{L}(z) \nabla E(z) + \nabla E(z) \cdot \boldsymbol{M}(z) \nabla S(z) = 0, \tag{4}$$

i.e., one ensures the conservation of energy in closed systems.

Equivalently,

$$\dot{S}(z) = \nabla s(z) \cdot \dot{z} = \nabla S(z) \cdot \boldsymbol{L}(z) \nabla E(z) + \nabla S(z) \cdot \boldsymbol{M}(z) \nabla S(z) \geq 0, \tag{5}$$

which ensures the fulfillment of the second principle of thermodynamics.

The reason for choosing GENERIC as the starting paradigm for this work is therefore obvious: it guarantees two basic principles such as the conservation of energy and the second principle of thermodynamics. It is under the umbrella of GENERIC that we will guarantee that the found laws will respect basic principles of utmost importance (such as the symmetries of the system, see [11]) and that, after this identification, the resulting time integration schemes will show the right conservation properties [14].

However, it is important to note that the choice of the state space of the system, z, is not obvious. First, the chosen variables must be measurable experimentally, of course. Otherwise, the identification of the system will be complicated. Secondly, and perhaps more importantly, not every possible description of a system can be cast into the GENERIC framework. For systems obeying the classical laws of mechanics, the most detailed (yet often very impractical) level of description is that of molecular dynamics. By successively coarse-graining the system, keeping in the description those variables that evolve in a slow manifold, one arrives, in the limit, at a description in which the sole variables that are involved are those that are conserved in the system along time, i.e., one arrives at the thermodynamics description of the system. During this journey, different descriptions are possible, and not all are suitable for a GENERIC structure [16]. In general, however, GENERIC seems to be the right framework to express a set of equations yet to be found by means of fitting of experimental results. It involves the most general variables of the system, energy and entropy, while ensuring the satisfaction of the most general requirements of thermodynamics.

However, the proposed methodology, which will be clear in the following section, does not look for the identification of a constitutive equation. Instead, what we propose is to work in a purely numerical, discrete way. In [10], we proposed the concept of *constitutive manifold*, by assuming that the experimental results (typically twelve-dimensional stress–strain couples for solid mechanics or stress–strain rates for fluid mechanics) live in a certain manifold $\mathcal{M}$ whose structure is to be identified, possibly with manifold learning techniques. Once identified, the structure of $\mathcal{M}$ will allow for an algorithmic numerical approximation of tangent moduli with which to operate in a purely discrete manner (see also [17]).

3 The proposed identification algorithm

It is assumed that the available data will provide the necessary information so as to reconstruct the state of the system at discrete time steps. In other words, we assume to know in advance a set of $n_{\texttt{meas}}$ vector-valued measurements of the already mentioned variables of interest $Z = \{z_0, z_1, \ldots, z_{n_{\texttt{meas}}}\}$. By discretizing Eq. (2), one arrives at

$$\frac{z_{n+1} - z_n}{\Delta t} = \mathsf{L}(z_{n+1})\mathsf{DE}(z_{n+1}) + \mathsf{M}(z_{n+1})\mathsf{DS}(z_{n+1}), \tag{6}$$

where, for simplicity, we denoted $z_{n+1} = z_{t+\Delta t}$ and where L and M are the discrete version of the Poisson and friction operators, respectively. In turn, DE and DS represent the discrete gradients. In general, matrix L is constant over the process, while matrix M frequently varies.

The proposed governing equation identification algorithm will therefore consist of the identification of the discrete values L and M, on one hand, and DE and DS, on the other. In sharp contrast to previous works, such as [6,7], we do not pursue the identification of a particular term (such as polynomials, sinus and cosinus) in the law. Instead, we will approximate the mentioned ingredients L, M, DE and DS numerically and construct with them the already introduced *constitutive manifold* (see [10,17,18]).

Within the realm of variational data assimilation, we will assume that the experimental measurements in Z are exact [19,20]. Of course, data will always be corrupted by noise to some extent, and this will oblige us to consider z in a Bayesian framework. This can be done by stating Eq. (2) in the framework of a Fokker–Planck equation, which is always possible [21]. This is currently the focus of our investigations and will be published elsewhere.

It is worth noting that by identifying the particular form of $E(z)$ we are doing no other thing than identifying what we usually call the "constitutive law" in solid mechanics. In the hyperelasticity framework, we usually denote by ψ or W the strain energy density function and obtain some stress measure (usually the second Piola–Kirchhoff tensor) by means of the computation of the gradient of the elastic energy with respect to some strain measure. In a hyperelastic context, we deal with purely conservative systems, and this will be therefore equivalent to obtaining the Poisson matrix and the $\nabla E(z)$ terms.

Therefore, the proposed algorithm will consist in solving the following (possibly constrained) minimization problem within a time interval $\mathcal{J} \subseteq \mathcal{I}$:

$$\boldsymbol{\mu}^* = \{\mathsf{L}, \mathsf{M}, \mathsf{DE}, \mathsf{DS}\} = \arg\min_{\boldsymbol{\mu}} ||z(\boldsymbol{\mu}) - z^{\mathtt{meas}}||, \tag{7}$$

with $z^{\mathtt{meas}} \subseteq Z$, a subset of the total available experimental results. Since L, M, DE, DS will in general be dependent on z, the choice of the size of $z^{\mathtt{meas}}$ deserves also some analysis: global fits will in general lead to excessive smoothing of the identified results, while using too small experimental sets will lead to ill-posed minimization problems.

The general form of matrix L is very easy to find, in general—see the examples that follow—while the structure of M is frequently much more intricate. This is why we prefer, in general, to assume L known (if its form can be determined beforehand) and simplify the problem a bit and to re-formulate it as

$$\boldsymbol{\mu}^* = \{\mathsf{M}, \mathsf{DE}, \mathsf{DS}\} = \arg\min_{\boldsymbol{\mu}} ||z(\boldsymbol{\mu}) - z^{\mathtt{meas}}||, \tag{8}$$

so that only the structure of M and the discrete gradients is sought. This avoids to take into consideration all the constraints related to the skew symmetry of L and improves the convergence of the proposed algorithm.

By assuming z approximated in a finite element sense, gradient operators can straightforwardly be cast in matrix form as

$$\mathsf{DE} = \boldsymbol{A}z, \tag{9a}$$

$$\mathsf{DS} = \boldsymbol{B}z, \tag{9b}$$

where $\boldsymbol{A}$ and $\boldsymbol{B}$ represent the discrete, matrix form of the gradient operators leading to DE and DS, respectively.

Once identified, the manifold structure of $\{\mathsf{L}, \mathsf{M}, \mathsf{DE}, \mathsf{DS}\}$ will also serve to construct, following Eq. (6), energy-conserving integration schemes with non-decreasing entropy (see [14]).

At this point, several identification strategies can be envisaged. These are summarized next.

3.1 Identification strategies

To solve problem (8), several strategies could be implemented, depending on the usage of monolithic or staggered approaches, constrained or not.

3.1.1 Monolithic versus staggered approaches

For some systems, it is possible to easily design experiments under conservative (purely Hamiltonian) conditions. For instance, some systems can be isolated so as to obtain isothermal results with whom to identify the Poisson term of the GENERIC form of the model. Subsequent non-equilibrium experiments will help to identify the dissipative structure of the system. Of course, this is not always possible. One of such examples is that of viscoelastic materials. Viscous and elastic (purely conservative) parts of their behavior cannot be decoupled experimentally. In those cases, the whole set of ingredients of the GENERIC formalism must be identified at once.

3.1.2 Total versus partial identification

We have already mentioned that although Eq. (8) incorporates the four ingredients of GENERIC to be identified (i.e., L, M, DE, DS), some of these matrices are easily identified without resorting to any experimental result. For instance, if the system is of mechanical nature and purely Hamiltonian, by choosing $\boldsymbol{z} = \{\boldsymbol{q}(t), \boldsymbol{p}(t)\}$ (position and momentum of each degree of freedom), the Poisson matrix takes always the form

$$\boldsymbol{L}(\boldsymbol{z}) = \begin{pmatrix} \mathbf{0} & \mathbf{1} \\ \mathbf{-1} & \mathbf{0} \end{pmatrix}. \tag{10}$$

This is the case very often. In other situations, very simple considerations shed light on the form of $\boldsymbol{L}$ and—less frequently—of $\boldsymbol{M}$.

3.1.3 Constrained or unconstrained minimization

As mentioned before, one of the salient features of GENERIC is the guaranteed conservation of energy and positive entropy production, see Eqs. (4), (5). In order to identify the form of the discrete gradient operators, DE, DS, two possibilities arise: to verify *a posteriori* that the numerically identified terms fulfill these requirements, or to impose it *a priori*, by solving a constrained minimization procedure:

$$\boldsymbol{\mu}^* = \{\mathsf{M}, \mathsf{DE}, \mathsf{DS}\} = \arg\min_{\boldsymbol{\mu}} ||\boldsymbol{z}(\boldsymbol{\mu}) - \boldsymbol{z}^{\mathtt{meas}}||, \tag{11a}$$

$$\text{subject to:} \quad \boldsymbol{L} \cdot \boldsymbol{B}\boldsymbol{z} = \mathbf{0}, \tag{11b}$$

$$\boldsymbol{M} \cdot \boldsymbol{A}\boldsymbol{z} = \mathbf{0}, \tag{11c}$$

where restrictions (11b) and (11c) will help, in general, to facilitate the identification procedure while ensuring the thermodynamic consistency of the resulting model.

4 Results

To validate the proposed methodology, we begin by considering two different finite-dimensional problems whose GENERIC structure is known, so as to be able to determine its degree of accuracy. This allows us to determine the best strategies in order to minimize errors in the identification procedure. Then, an infinite-dimensional problem is analyzed that also proves the validity of the suggested strategy.

4.1 Simple pendulum

The first problem corresponds to a simple pendulum whose purely Hamiltonian structure, in the absence of any dissipation, responds to Eq. (10). Therefore, only the discrete matrix form of the gradient, $\boldsymbol{A}$, was identified.

The accuracy of the proposed identification method was tested by reproducing the dynamics of the system, integrated by constructing the time integrators proposed in [14], namely the simple scheme outlined by Eq. (6). As can be noticed, the agreement is almost perfect. Knowing in advance the form of $\boldsymbol{L}$, the identification of $\boldsymbol{A}$ employing all the available data (241 time increments) leads to an error vanishing to machine precision (see Fig. 1).

On the contrary, if the identification procedure is applied by taking subsets of five experimental measurements, an error in L2-norm of 0.049% was obtained (see Fig. 2).

4.2 Thermoelastic pendulum

As an example of a non-equilibrium problem to start with, we have chosen a problem presented in [14]. The system consists of two pendula connected by thermoelastic springs. Two masses m_1 and m_2 are thus connected by springs of internal energy e_1 and e_2 and are allowed to oscillate around a fixed point (see Fig. 3). We employ

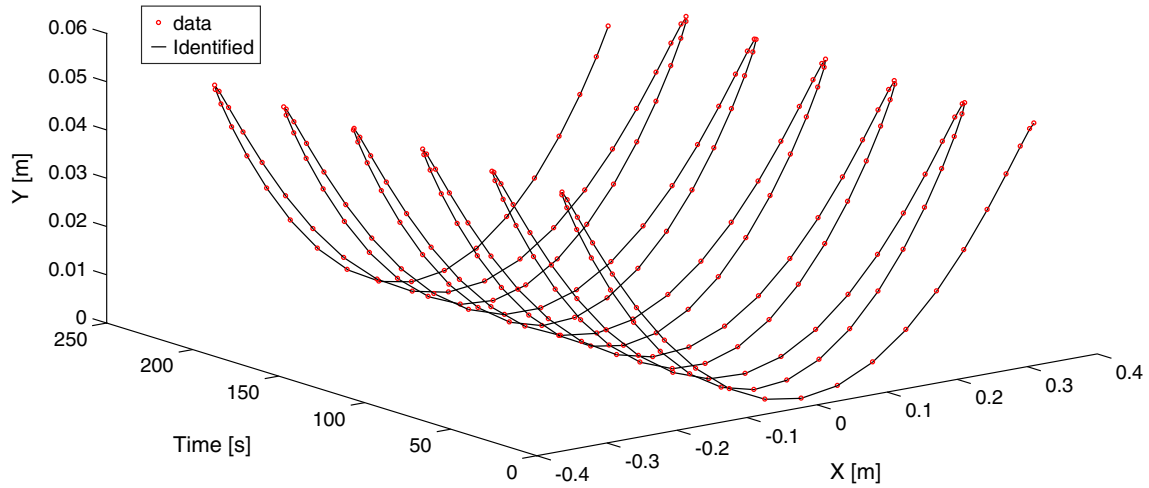

Fig. 1 Results for the pendulum problem. Data (circles) versus numerical integration of the identified system

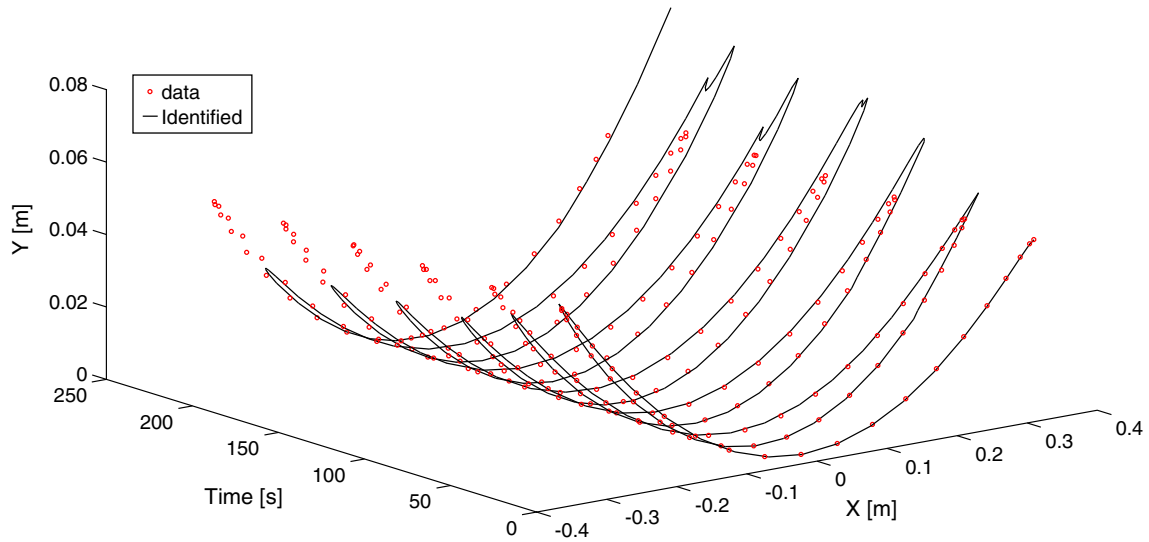

Fig. 2 Results for the pendulum problem. Data (circles) versus numerical integration of the identified system when the identification procedure is applied every five time increments

the classical notation of $\boldsymbol{q}_i$, $\boldsymbol{p}_i$, $i = 1, 2$ for position and momenta, respectively. In turn, springs have entropies s_j and longitudes at rest λ_j^0, $j = a, b$. Under this perspective, the state space of the system can be defined as

$$\mathcal{S} = \{z = (\boldsymbol{q}_1, \boldsymbol{q}_2, \boldsymbol{p}_1, \boldsymbol{p}_2, s_1, s_2) \in (\mathbb{R}^2 \times \mathbb{R}^2 \times \mathbb{R}^2 \times \mathbb{R}^2 \times \mathbb{R} \times \mathbb{R}), \boldsymbol{q}_1 \neq \boldsymbol{0}, \boldsymbol{q}_2 \neq \boldsymbol{q}_1\}.$$

The GENERIC structure of the problem will naturally involve the internal energy of the system, as already discussed. It can be computed as the sum of the kinetic energy (coming from the movement of the masses) and the potential energy in the springs, i.e.,

$$E(z) = K_1(z) + K_2(z) + e_a(\lambda_a, s_a) + e_b(\lambda_b, s_b),$$

where

$$\lambda_a = \sqrt{\boldsymbol{q}_1 \cdot \boldsymbol{q}_1}, \quad \lambda_b = \sqrt{(\boldsymbol{q}_2 - \boldsymbol{q}_1) \cdot (\boldsymbol{q}_2 - \boldsymbol{q}_1)}.$$

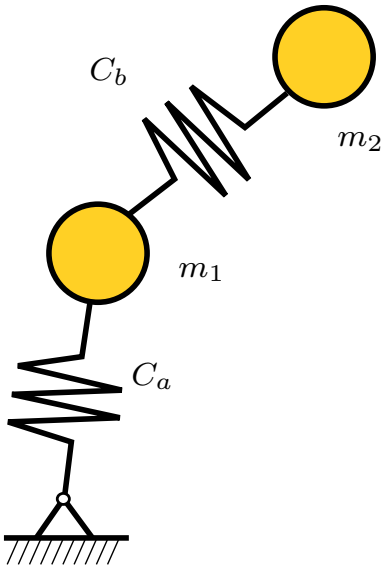

Fig. 3 Double thermal pendulum

It is assumed that the temperature in the springs, θ_j, changes due to the Joule effect, giving rise to

$$\theta_j = \frac{\partial e_j}{\partial s_j}, \quad j = a, b.$$

Assuming a conductivity κ in the springs, the resulting equations of the system will be

$$\begin{aligned}
\dot{\boldsymbol{q}}_i &= \frac{\boldsymbol{p}_i}{m_i}, \\
\dot{\boldsymbol{p}}_i &= -\frac{\partial}{\partial \boldsymbol{q}_i}(e_a + e_b), \\
\dot{s}_j &= \kappa \left(\frac{\theta_k}{\theta_j} - 1 \right),
\end{aligned}$$

with $i = 1, 2$, $j = a, b$, $k \neq j$. This gives rise to the following gradients, which are to be identified,

$$\begin{aligned}
\nabla E(z) &= \left(f_a \boldsymbol{n}_a - f_b \boldsymbol{n}_b, f_b \boldsymbol{n}_b, \frac{\boldsymbol{p}_1}{m_1}, \frac{\boldsymbol{p}_2}{m_2}, \theta_a, \theta_b \right), \\
\nabla S(z) &= (\boldsymbol{0}, \boldsymbol{0}, \boldsymbol{0}, \boldsymbol{0}, 1, 1),
\end{aligned}$$

with f_j, $\boldsymbol{n}_j$, $j = a, b$, the forces in the springs and their respective unit vector along their direction. Note that we assume them unknown and employ these expressions as ground truth just to test the accuracy of the proposed methodology.

Something which is particularly appealing from the structure of GENERIC, already commented in Introduction, is that different choices of state-space variables are equally valid. For instance, one can imagine

$$\mathcal{S} = \{z \mid z = (\boldsymbol{q}_1, \boldsymbol{q}_2, \boldsymbol{p}_1, \boldsymbol{p}_2, e_1, e_2)\},$$

or even

$$\mathcal{S} = \{z \mid z = (\boldsymbol{q}_1, \boldsymbol{q}_2, \boldsymbol{p}_1, \boldsymbol{p}_2, \theta_1, \theta_2)\},$$

and it will produce equivalent results (although with different complexities in the resulting expressions, see [14]).

Table 1 Errors (L2-norm) for the double thermal pendulum

	Strategy			
	Staggered		Monolithic	
	84 points (%)	17 points (%)	167 points (%)	34 points (%)
Constrained	0.000001	0.0684	0.0023	0.3072
Unconstrained	0.000018	0.3114	0.00036	0.0399

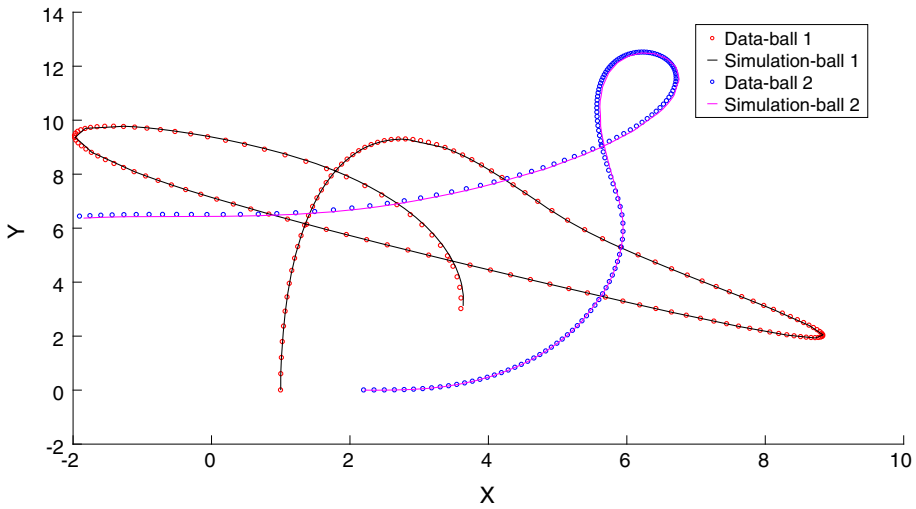

Fig. 4 Results for the thermal pendulum problem. Trajectories of the two masses. Data (circles) versus numerical integration of the identified system. Monolithic identification on sets of $|z^{\text{meas}}| = 34$ data points

Under the first of the choices, Poisson and friction matrices will result in

$$\boldsymbol{L}(z) = \begin{pmatrix} \mathbf{0} & \mathbf{0} & \mathbf{1} & \mathbf{0} & \mathbf{0} & \mathbf{0} \\ \mathbf{0} & \mathbf{0} & \mathbf{0} & \mathbf{1} & \mathbf{0} & \mathbf{0} \\ \mathbf{-1} & \mathbf{0} & \mathbf{0} & \mathbf{0} & \mathbf{0} & \mathbf{0} \\ \mathbf{0} & \mathbf{-1} & \mathbf{0} & \mathbf{0} & \mathbf{0} & \mathbf{0} \\ \mathbf{0} & \mathbf{0} & \mathbf{0} & \mathbf{0} & 0 & 0 \\ \mathbf{0} & \mathbf{0} & \mathbf{0} & \mathbf{0} & 0 & 0 \end{pmatrix}, \quad \boldsymbol{M}(z) = \begin{pmatrix} \mathbf{0} & \mathbf{0} & \mathbf{0} & \mathbf{0} & \mathbf{0} & \mathbf{0} \\ \mathbf{0} & \mathbf{0} & \mathbf{0} & \mathbf{0} & \mathbf{0} & \mathbf{0} \\ \mathbf{0} & \mathbf{0} & \mathbf{0} & \mathbf{0} & \mathbf{0} & \mathbf{0} \\ \mathbf{0} & \mathbf{0} & \mathbf{0} & \mathbf{0} & \mathbf{0} & \mathbf{0} \\ \mathbf{0} & \mathbf{0} & \mathbf{0} & \mathbf{0} & \kappa \frac{\theta_b}{\theta_a} & -\kappa \\ \mathbf{0} & \mathbf{0} & \mathbf{0} & \mathbf{0} & -\kappa & \kappa \frac{\theta_a}{\theta_b} \end{pmatrix},$$

although, as explained before, we assume $\boldsymbol{M}$ unknown.

The different identification procedures suggested in Sect. 3 allowed to determine the precise form of the gradients of energy and entropy, respectively. Errors in the numerical reconstruction of the pendula trajectories with the just identified terms are reported in Table 1. In that table, the mentioned number of points refers to the size of data sets employed for the identification, i.e., the size of the set z^{meas} in Eq. (8).

An example of the reconstructed trajectory of the masses is shown in Fig. 4.

4.3 Oldroyd-B fluid

The field of non-Newtonian fluid mechanics is where GENERIC originated and one of the most active in terms of identification of complex constitutive equations. The Oldroyd-B fluid model is a clear example of an equation that can be derived by starting from very different assumptions: from continuum considerations to coarse-graining microscopical descriptions or, finally, by employing a Fokker–Planck probabilistic description [22].

The Oldroyd-B model originated as a means to model the flow of diluted polymeric solutions. These polymer chains can be considered both from a purely macroscopic point of view and from a microscopic one, by modeling them as linear dumbbells in a Newtonian medium. From a purely continuum point of view, the

constitutive equation of an Oldroyd-B fluid arises from considering the deviatoric part $\boldsymbol{T}$ of the stress tensor $\boldsymbol{\sigma}$ (the so-called extra-stress tensor) of the form,

$$\boldsymbol{T} + \lambda_1 \overset{\triangledown}{\boldsymbol{T}} = \eta_0 \left(\dot{\boldsymbol{\gamma}} + \lambda_2 \overset{\triangledown}{\dot{\boldsymbol{\gamma}}} \right), \tag{12}$$

where the triangle denotes the nonlinear upper-convected derivative introduced by Oldroyd [23]. The coefficients η_0, λ_1 and λ_2 are material constants. Finally, following standard notation, $\dot{\boldsymbol{\gamma}} = (\nabla^s \boldsymbol{v}) = \boldsymbol{D}$ represents the strain rate tensor.

If we now consider separately the stress in the solvent (denoted by a subscript s) and polymer (denoted by a subscript p) components as

$$\boldsymbol{T} = \eta_s \dot{\boldsymbol{\gamma}} + \boldsymbol{\tau},$$

this gives rise to

$$\boldsymbol{\tau} + \lambda_1 \overset{\triangledown}{\boldsymbol{\tau}} = \eta_p \dot{\boldsymbol{\gamma}},$$

which is the constitutive equation for the elastic stress.

An alternative derivation can be obtained by starting from a population of linear dumbbells immersed in a Newtonian fluid [24]. What is here intended is to take the Oldroyd-B model as a paradigm of a class of viscoelastic (and therefore non-Hamiltonian) fluids that encompasses both macroscopic and mesoscopic models. Therefore, we assume that we have a set of pseudo-experimental measurements arising from an Oldroyd-B fluid and try first to identify its constitutive equation in a GENERIC framework and, second, to reconstruct the results by integrating the just found constitutive equations by means of Eq. (6).

4.3.1 GENERIC form of the problem

In a GENERIC framework, rather than dealing with constitutive equations for the (elastic) extra-stress tensor, as one intuitively usually starts by, it is often suggested (see, for instance, [25] and references therein) to start by using the conformation tensor $\boldsymbol{c} = \langle \boldsymbol{r}\boldsymbol{r} \rangle$, as the second moment of the dumbbell end-to-end distance distribution function. In fact, this choice allows for a natural introduction of thermal fluctuations in the model [26]. It can be demonstrated that for modeling viscoelastic fluids, the only variables needed to describe the state of the system are the momentum density $\boldsymbol{p} = \rho \boldsymbol{v}$ and the conformation density, $\hat{\boldsymbol{c}} = \rho c_p \boldsymbol{c}$, where $\boldsymbol{v}$ represents the fluid's velocity, ρ is the density and c_p is the number of polymer molecules per unit mass (see [27] and references therein). This choice can result somewhat unnatural for scientists used to continuum models. And indeed it is, if one takes into account that the conformation tensor is not easily observable from an experimental point of view. However, the reader can easily notice its similitude to the left Cauchy–Green or Finger strain tensor $\boldsymbol{b} = \boldsymbol{F} \cdot \boldsymbol{F}^T$. Indeed, in a cross-linked rubber, $\boldsymbol{c} = N\ell^2 \boldsymbol{b}/3$, where N is the number of statistical segments in a polymer chain and ℓ its length [25].

It is well known that the extra-stress tensor takes the form

$$\boldsymbol{\tau} = -\frac{n}{2\zeta_{12}} \overset{\triangledown}{\boldsymbol{c}},$$

i.e., it is in fact proportional to the convective (or Oldroyd) derivative of the conformation tensor. This magnitude is more suitable as a characteristic internal variable of the fluid than $\boldsymbol{c} = \langle \boldsymbol{r}\boldsymbol{r} \rangle$ itself.

Therefore, in order to model a viscoelastic fluid in the GENERIC framework, we must consider, for each of the M fluid particles that compose the (discretized) fluid, their position $\boldsymbol{r}_j$, velocity $\boldsymbol{v}_j$, energy E_j and extra-stress tensor $\boldsymbol{\tau}_j$. The internal energy E_j includes, of course, the kinetic energy contribution from the solvent and the beads, plus the potential energy of solvent–solvent, solvent–bead and bead–bead interaction. Each one of the M fluid particles is assumed to contain $j = 1, 2, \ldots, N$ dumbbells and, of course, an entropy $S_j(E_j, \boldsymbol{\tau}_j, V_j)$, with V_j the volume associated with each particle.

Therefore, using the previous notation, the set of variables employed to describe the phase space of the fluid will be

$$\mathcal{S} = \{ z = (\boldsymbol{r}_j, \boldsymbol{v}_j, E_j, \boldsymbol{\tau}_j, j = 1, 2, \ldots, M) \in (\mathbb{R}^2 \times \mathbb{R}^2 \times \mathbb{R} \times \mathbb{R}^4)^M \}. \tag{13}$$

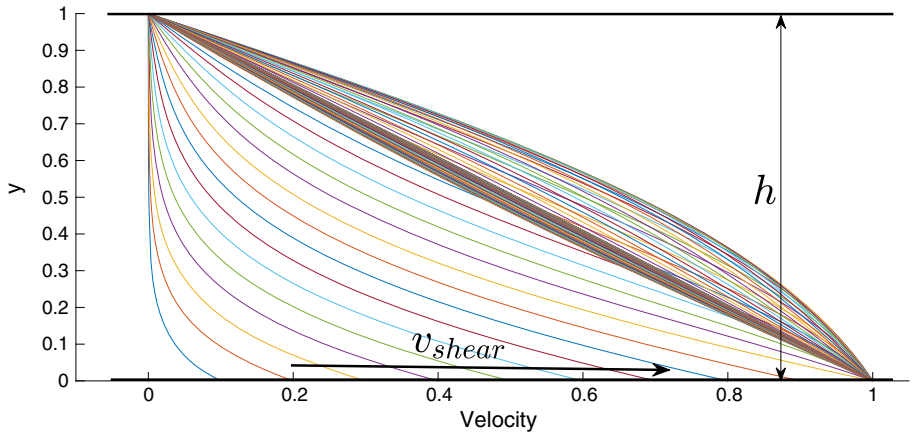

Fig. 5 Velocity profile at every $\Delta t = 0.01$ seconds ($t \in (0, 1.5]$) for the start-up of a Couette flow (shear flow between two plates, typical of a rheometer). In this case, velocity is imposed at the bottom plate, with $h = 1.0$ and $v_{\text{shear}} = 1.0$. Notice the *overshoot* of the velocity profile just before the permanent regime (linear velocity profile)

4.3.2 Implementation details

Although the just introduced strategy is entirely equivalent to the existing data-driven simulation approaches by Ortiz and coworkers [9,28], in the sense that it performs a constrained minimization problem at every integration point, alternative approaches exist. Instead of fitting point-wise the *best* possible constitutive values provided by data, it is possible to do it in a non-local manner, by employing model order reduction approaches.

Model reduction consists, essentially, in finding the slow manifold in which the system evolves. Therefore, for a (full order) problem formulated under the GENERIC paradigm, ensuring that its reduced-order version also verifies the GENERIC structure is not obvious. The interested reader can consult [29]. The obvious advantage is the drastic reduction in the number of degrees of freedom.

In this case, we employed a very simple strategy based on the employ of the proper orthogonal decomposition (POD) of the pseudo-experimental results [30–32]. An alternative, perhaps more accurate, is to employ some form of nonlinear dimensionality reduction, or manifold learning strategy, as in [33].

Our pseudo-experimental results were generated with a CONNFFESSIT approach [34,35] to the problem of a Couette flow of an Oldroyd-B fluid. The Couette flow is the pure shear flow between two rigid plates produced typically in rheometers, and thus the most frequent form of experimental results for this type of fluids. The CONNFFESSIT approach combines finite elements and stochastic techniques for the solution of micro-macro- flows of viscoelastic flows.

Given the rheometric character of the flow (in other words, its homogeneous character), the code discretizes only the one-dimensional distance h between the rheometer plates, by employing one hundred finite elements (and, consequently, 101 nodes). We consider the start-up of a flow with a Reynolds number of 0.1 and Weissenberg number 0.5. Each finite element node is equipped with 10,000 dumbbells.

A simple proper orthogonal decomposition (POD) of the 150 *snapshots* of the velocity profile (see Fig. 5) revealed that the flow can be expressed in terms of a few degrees of freedom (see Fig. 6). In fact, only six modes produce a decay on the eigenvalues of more than four orders of magnitude. Therefore, instead of the 101 nodes employed to build the mesh, our identification procedure employed the just mentioned six degrees of freedom.

Thus, for each of the six retained degrees of freedom, the Poisson and friction matrices are known to have the form

$$\boldsymbol{L}_k(z) = \begin{pmatrix} 0 & 1 & 0 & 0 \\ -1 & 0 & 1 & -1 \\ 0 & -1 & 0 & 0 \\ 0 & 1 & 0 & 0 \end{pmatrix}, \quad \boldsymbol{M}_k(z) = \begin{pmatrix} 0 & 0 & 0 & 0 \\ 0 & 1 & 1 & 0 \\ 0 & 1 & 1 & 0 \\ 0 & 0 & 0 & 1 \end{pmatrix}, k = 1, \ldots, \mathtt{n}_{\text{POD}},$$

with $\mathtt{n}_{\text{POD}}$ the number of employed POD modes. They are, however, assumed unknown, and their form is determined by the proposed method. In this case, the identification includes both $\boldsymbol{L}$ and $\boldsymbol{M}$ without any significant difficulty.

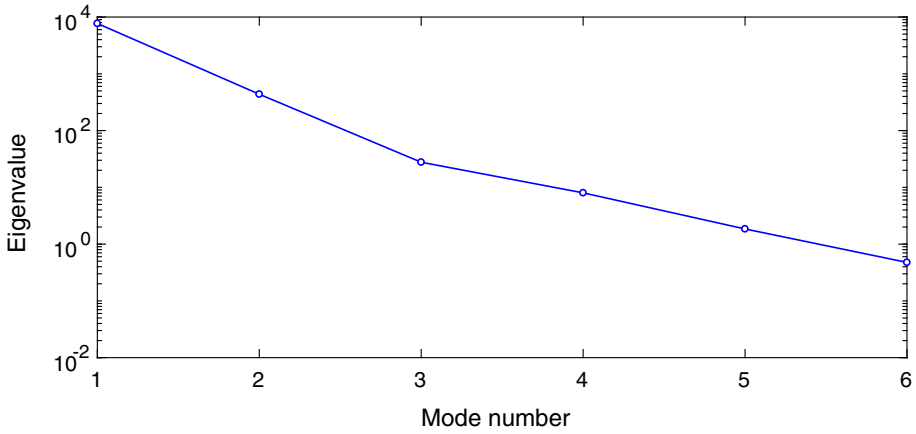

Fig. 6 POD modes and related eigenvalues for the Couette flow

Note that, due to the particular form of the Couette flow, the variables in $\mathcal{S}$ (see Eq. (13)) turn out to be one-dimensional and hence the 4×4 size of the Poisson and friction matrices.

With these ingredients, the pseudo-experimental and identified results for nodes $1, 11, \ldots, 101$ along the vertical axis of the flow are represented in Fig. 7.

As in previous examples, the accuracy of the proposed methods depends on the number of time samples employed to perform the minimization problem. In this case, by performing a constrained minimization (thus enforcing conservation of energy and strictly positive entropy dissipation) with sets of 150 snapshots, the error in the velocity field turned out to be of 10^{-8}. The unconstrained minimization strategy, on the contrary, was unable to find any suitable solution for the problem.

4.3.3 Numerical integration of an arbitrary flow

Of course, the final goal of this procedure is not to reproduce the experimental results but to be able to integrate different flow regimes once the constitutive manifold of the particular fluid has been identified. Assume, for simplicity, that we have identified the discrete gradient operators at time t_n, $\mathsf{DE} = \boldsymbol{A}_n z_n$ and $\mathsf{DS} = \boldsymbol{B}_n z_n$, and the Poisson and friction matrices L and M, respectively—that turned out to be constant for this problem—for two flows under different conditions, say Weissenberg, We, numbers. We have, therefore, the values L, M and the triplets $\boldsymbol{A}_n^1$, $\boldsymbol{B}_n^1$, z_n^1 and $\boldsymbol{A}_n^2$, $\boldsymbol{B}_n^2$, z_n^2, together with the current state of the system, z_n. The objective is then to numerically integrate, without any explicit knowledge on the constitutive equations of an Oldroyd-B fluid, the state equations for the flow under a third We value, characterized by $\boldsymbol{A}^{\text{obj}}$, $\boldsymbol{B}^{\text{obj}}$. Assume known the value of the weights w_1 and w_2 that will make Eq. (6) hold under the new flow conditions, namely,

$$\begin{aligned} z_{n+1}^{\text{obj}} &= z_n + \Delta t \cdot \left[\boldsymbol{L}\boldsymbol{A}^{\text{obj}} + \boldsymbol{M}\boldsymbol{B}^{\text{obj}}\right] z_n \\ &= z_n + w_1 \Delta t \cdot \left[\boldsymbol{L}\boldsymbol{A}_n^1 + \boldsymbol{M}\boldsymbol{B}_n^1\right] z_n^1 \\ &\quad + z_n + w_2 \Delta t \cdot \left[\boldsymbol{L}\boldsymbol{A}_n^2 + \boldsymbol{M}\boldsymbol{B}_n^2\right] z_n^2 \end{aligned}$$

with $\boldsymbol{L}$ and $\boldsymbol{M}$ also known. Some simple algebra leads to the following conditions:

$$\begin{aligned} \boldsymbol{A}^{\text{obj}} z_n &= w_1 \boldsymbol{A}_n^1 z_n^1 + w_2 \boldsymbol{A}_n^2 z_n^2, \\ \boldsymbol{B}^{\text{obj}} z_n &= w_1 \boldsymbol{B}_n^1 z_n^1 + w_2 \boldsymbol{B}_n^2 z_n^2. \end{aligned}$$

Computing the interpolating weights $w_1, w_2, \ldots, w_\ell$, with ℓ the number of neighboring experimental results to interpolate with, can be done, for instance, by resorting to nonlinear dimensionality reduction techniques such as locally linear embedding (LLE), which produces these weights as a by-product of the dimensionality reduction process [36].

By doing so, the results of integrating a Couette flow at $We = 0.75$ from the experimental results obtained at $We = 0.5$ and $We = 1.0$ (thus, $w_1 = w_2 = 0.5$ in a straightforward manner, for this simple illustration) are shown in Fig. 8. In it, the data-driven results (we recall again that no constitutive equation was employed

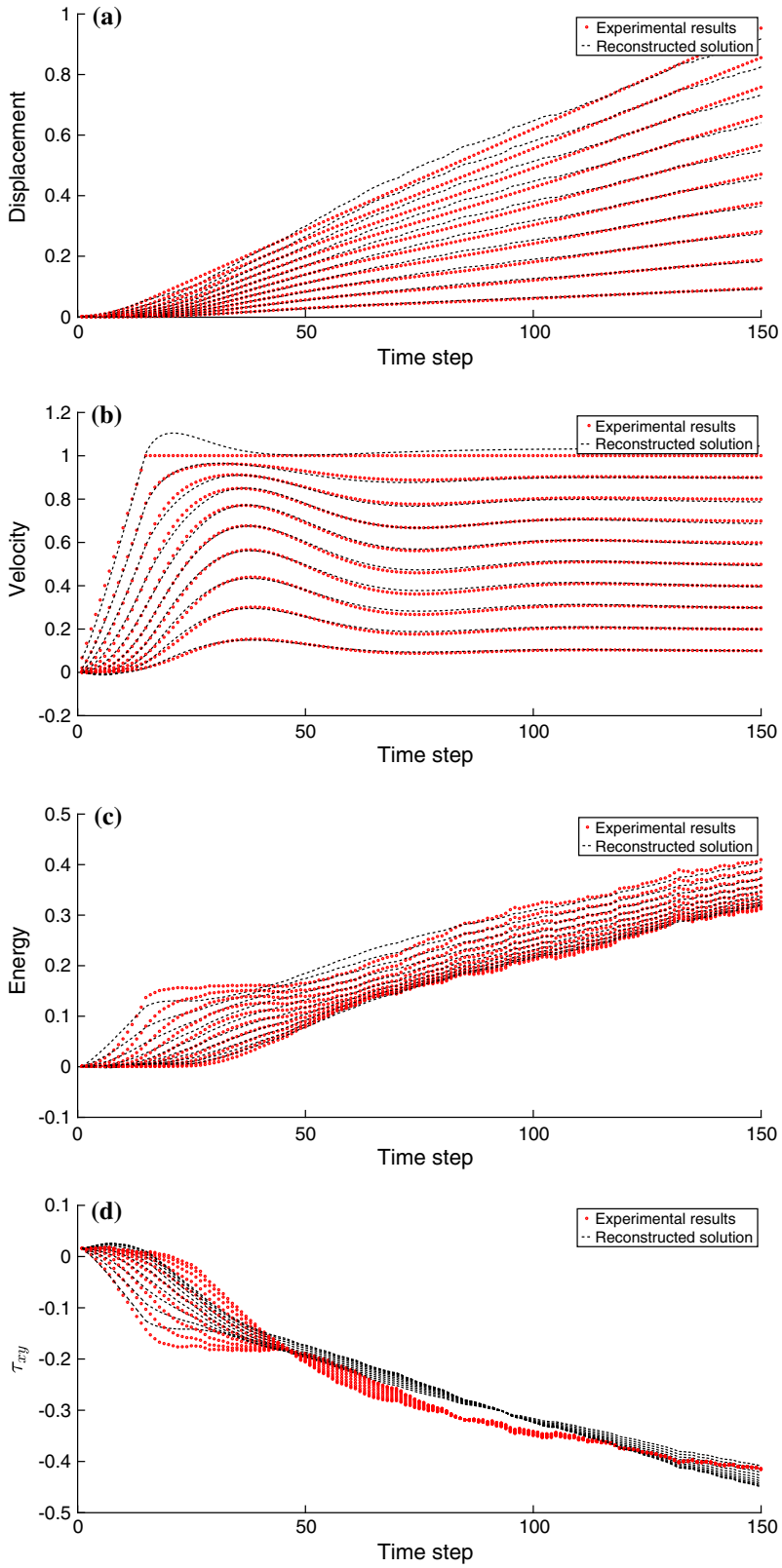

Fig. 7 Experimental versus reconstructed phase space variables for the Oldroyd-B fluid. **a** Displacement, **b** velocity, **c** energy and **d** xy component of the extra-stress tensor, τ_{xy}. Every variable is represented for nodes 1, 11, . . . , 101 along the height of the channel, h

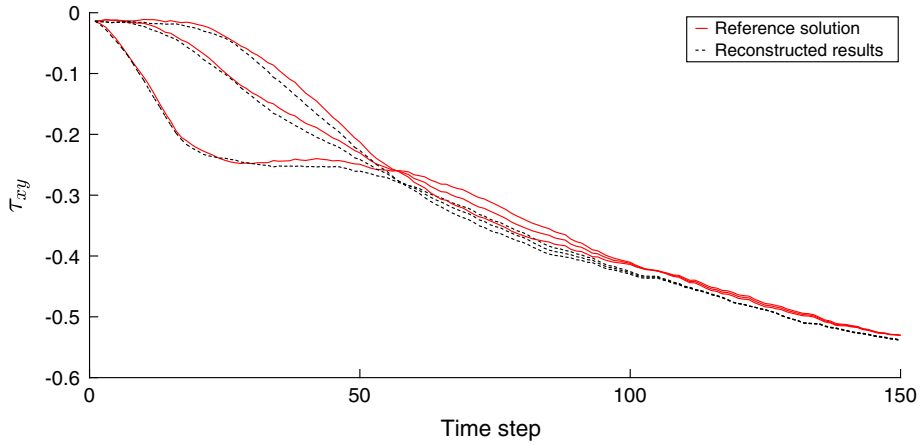

Fig. 8 Stress tensor component τ_{xy} evolution for the reconstructed flow versus reference solution. Results for the points at $y = 0$, $y = \frac{h}{2}$ and $y = h$ are shown

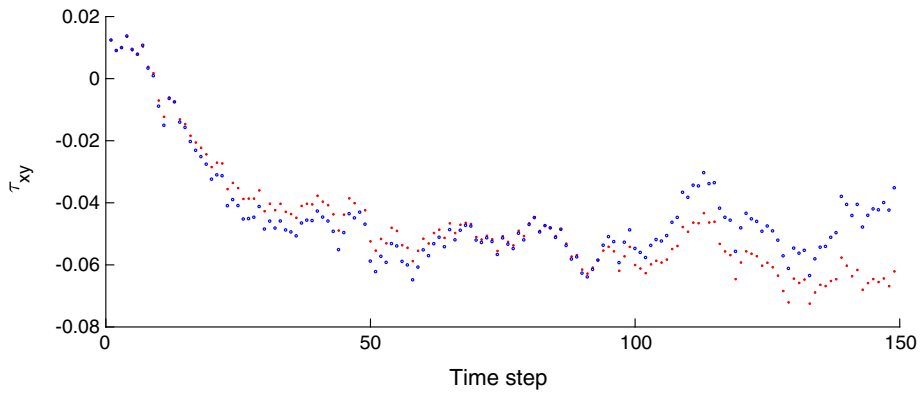

Fig. 9 Evolution of the τ_{xy} component for a given point in a Poiseuille flow. Red asterisks, reference values. Blue circles, obtained values

to perform the integration) are compared toward the result of a direct numerical integration. Results for the stress component τ_{xy} are shown. $L2$-norm error of the velocity field shown to be 0.4988% in this particular case.

4.3.4 Poiseuille flow

Obviously, the aim of the just developed technique is not to be able to reproduce experimental results. Rather, it is to be able to simulate situations for which no experimental result exist. Usually, rheologists employ rheometers to fully characterize the constitutive equations of a particular fluid. The simplest of these rheometers provokes simple shear (Couette) flows, as in the previous sections. In this section, we will try to demonstrate that, once the constitutive manifold has been properly characterize by means of the necessary experimental results, the approach just developed could be employed for the simulation of flows for which no previous result exists.

So, let us assume that we have performed enough experiments so as to characterize the constitutive manifold. In this case, we have simulated a big amount of shear (Couette) flows to characterize the fluid. With the help of these (pseudo-)experimental results, we are about to simulate the start-up of a Poiseuille flow. By taking a time increment of $\Delta t = 0.006$, we interpolate from the set of available (pseudo-)experimental results the $\boldsymbol{A}$ and $\boldsymbol{B}$ matrices that are employed to advance the flow in time. Figure 9 represents the evolution of the τ_{xy} component along time, for both the reference solution and the just computed one. For this flow, the mean relative error for this value is between 4.13 and 16.14% for the different nodes of the discretization (which is actually one-dimensional). Of course, these errors can be lowered by employing finer meshes and smaller time steps.

5 Discussion

Within the realm of data-intensive computational mechanics, this paper presents a novel methodology able to integrate the equations of motion without resorting to any constitutive equation (the so-called data-driven computational mechanics framework first established in [9]). The main novelty in the approach herein consist in the development of a thermodynamically consistent approach to the problem that guarantees the fulfillment of the first and second principles of thermodynamics, independently of the quality of the experimental results. This is in sharp contrast to existing approaches in the literature, either the ones working without any constitutive assumption (see [9,10,17,18]) or those that identify the form of the governing equations by choosing among a predefined set of equations, [6,7].

The present approach is based on the usage of the GENERIC paradigm, a framework that guarantees the strict energy conservation and positive entropy production, along with the symmetries of the system, and that generalizes the Hamiltonian form of classical mechanics to non-equilibrium systems. The proposed methodology thus identifies the proper GENERIC structure of the problem. The method identifies either the whole GENERIC structure composed by the Poisson and friction matrices of the problem, plus the precise numerical form of the gradients of the energy and entropy. However, for some complex problems it has been found that the form of the Hamiltonian and dissipative structures of the problem is easy to identify and that the method works considerably better by just finding the form of the gradients of energy and entropy, respectively. This is equivalent, of course, to finding in a numerical, point-wise manner, the form of the *constitutive manifold* that the authors defined in a previous work (see [10]).

But the proposed methodology not only provides with a suitable method to unveil the precise form of the Hamiltonian and dissipative structures of the problem. It also provides a robust and thermodynamically consistent way to integrate these equations without employing any constitutive equation (the so-called *data-driven computational mechanics* paradigm).

The aforementioned properties have been demonstrated by solving different problems: from simple pendulums with discrete degrees of freedom to complex viscoelastic fluids. In this last case, the proposed technique has been combined with a classical model order reduction technique (POD) that allows to highly simplify the problem and to greatly diminish the number of degrees of freedom and variables to identify.

Acknowledgements This work has been supported by the Spanish Ministry of Economy and Competitiveness through Grants number DPI2017-85139-C2-1-R and DPI2015-72365-EXP and by the Regional Government of Aragon and the European Social Fund, research group T88.

References

1. Bongard, J., Lipson, H.: Automated reverse engineering of nonlinear dynamical systems. Proc. Nat. Acad. Sci. **104**(24), 9943–9948 (2007)
2. Schmidt, M., Lipson, H.: Distilling free-form natural laws from experimental data. Science **324**(5923), 81–85 (2009)
3. Battista, A., Rosa, L., dell'Erba, R., Greco, L.: Numerical investigation of a particle system compared with first and second gradient continua: deformation and fracture phenomena*. Math. Mech. Solids **22**(11), 2120–2134 (2017)
4. Della Corte, A., Battista, A., dellIsola, F.: Referential description of the evolution of a 2d swarm of robots interacting with the closer neighbors: perspectives of continuum modeling via higher gradient continua. Int. J. Non-Linear Mech. **80**, 209–220 (2016)
5. Della Corte, A., Battista, A., dell'Isola, F.: Modeling Deformable Bodies Using Discrete Systems with Centroid-Based Propagating Interaction: Fracture and Crack Evolution, pp. 59–88. Springer, Berlin (2017)
6. Brunton, S.L., Proctor, J.L., Kutz, J.N.: Discovering governing equations from data by sparse identification of nonlinear dynamical systems. Proc. Nat. Acad. Sci. USA **113**(15), 3932–3937 (2016)
7. Peherstorfer, B., Willcox, K.: Data-driven operator inference for nonintrusive projection-based model reduction. Comput. Methods Appl. Mech. Eng. **306**, 196–215 (2016)
8. Daniels, B.C., Nemenman, I.: Automated adaptive inference of phenomenological dynamical models. Nat. Commun. **6**, 8133 EP (2015)
9. Kirchdoerfer, T., Ortiz, M.: Data-driven computational mechanics. Comput. Methods Appl. Mech. Eng. **304**, 81–101 (2016)
10. Ibañez, R., Abisset-Chavanne, E., Aguado, J.V., Gonzalez, D., Cueto, E., Chinesta, F.: A manifold learning approach to data-driven computational elasticity and inelasticity. Arch. Comput. Methods Eng. **25**, 1–11 (2016)
11. Oettinger, H.C.: Beyond Equilibrium Thermodynamics. Wiley, Hoboken (2005)
12. Grmela, M., Christian Öttinger, H.: Dynamics and thermodynamics of complex fluids. i. development of a general formalism. Phys. Rev. E **56**, 6620–6632 (1997)
13. Öttinger, H.C.: Nonequilibrium thermodynamics: a powerful tool for scientists and engineers. DYNA **79**, 122–128 (2012)
14. Romero, I.: Thermodynamically consistent time-stepping algorithms for non-linear thermomechanical systems. Int. J. Numer. Meth. Eng. **79**(6), 706–732 (2009)

15. Romero, I.: Algorithms for coupled problems that preserve symmetries and the laws of thermodynamics: Part i: monolithic integrators and their application to finite strain thermoelasticity. Comput. Methods Appl. Mech. Eng. **199**(25–28), 1841–1858 (2010)
16. Español, P.: Statistical Mechanics of Coarse-Graining, pp. 69–115. Springer, Berlin (2004)
17. Ibañez, R., Borzacchiello, D., Aguado, J.V., Abisset-Chavanne, E., Cueto, E., Ladeveze, P., Chinesta, F.: Data-driven non-linear elasticity. Constitutive manifold construction and problem discretization. Comput. Mech. **60**(5), 813–826 (2017)
18. Lopez, E., Gonzalez, D., Aguado, J.V., Abisset-Chavanne, E., Cueto, E., Binetruy, C., Chinesta, F.: A manifold learning approach for integrated computational materials engineering. Arch. Comput. Methods Eng. **25**, 1–10 (2016)
19. Manzoni, A., Lassila, T., Quarteroni, A., Rozza, G.: A reduced-order strategy for solving inverse bayesian shape identification problems in physiological flows. In: Hans Georg B., Xuan Phu H., Rolf R., Johannes P. Schlöder, (eds.) Modeling, Simulation and Optimization of Complex Processes—HPSC 2012: In: Proceedings of the Fifth International Conference on High Performance Scientific Computing, March 5–9, 2012, Hanoi, Vietnam, pp. 145–155. Springer International Publishing, Cham, (2014)
20. Sullivan, T.J.: Introduction to Uncertainty Quantification. Springer, Berlin (2015). [Texts in Applied Mathematics]
21. Soize, C.: The Fokker–Planck Equation for Stochastic Dynamical Systems and its Explicit Steady State Solutions, 17th edn. World Scientific, SIngapore (1994)
22. Owens, R.G., Phillips, T.N.: Computational Rheology. Imperial College Press, London (2002)
23. Walters, K., Webster, M.F.: The distinctive CFD challenges of computational rheology. Int. J. Numer. Meth. Fluids **43**(5), 577–596 (2003)
24. Owens, R.G., Phillips, T.N.: Computational Rheology. Imperial College PRess, London (2002)
25. Pasquali, Matteo., Scriven, L.E.: Theoretical modeling of microstructured liquids: a simple thermodynamic approach. *Journal of Non-Newtonian Fluid Mechanics*, 120(1):101 – 135, (2004). 3rd International workshop on Nonequilibrium Thermodynamics and Complex Fluids
26. Vázquez-Quesada, A., Ellero, M., Español, P.: Consistent scaling of thermal fluctuations in smoothed dissipative particle dynamics. J. Chem. Phys. **130**(3), 034901 (2009)
27. Mavrantzas, V.G., Christian Öttinger, H.: Atomistic monte carlo simulations of polymer melt elasticity: their nonequilibrium thermodynamics generic formulation in a generalized canonical ensemble. Macromolecules **35**(3), 960–975 (2002)
28. Kirchdoerfer, T., Ortiz, M.: Data driven computing with noisy material data sets. Comput. Methods Appl. Mech. Eng. **326**, 622–641 (2017)
29. Christian Öttinger, H.: Preservation of thermodynamic structure in model reduction. Phys. Rev. E **91**, 032147 (2015)
30. Karhunen, K.: Uber lineare methoden in der wahrscheinlichkeitsrechnung. Ann. Acad. Sci. Fennicae, ser. Al. Math. Phys., 37, (1946)
31. Loève, M.M.: Probability theory. The University Series in Higher Mathematics, 3rd edn. Van Nostrand, Princeton, NJ (1963)
32. Lorenz, E.N.: Empirical Orthogonal Functions and Statistical Weather Prediction. MIT, Department of Meteorology, Scientific Report Number 1, Statistical Forecasting Project, (1956)
33. Millán, D., Arroyo, M.: Nonlinear manifold learning for model reduction in finite elastodynamics. Comput. Methods Appl. Mech. Eng. **261–262**, 118–131 (2013)
34. Laso, M., Öttinger, H.C.: Calculation of viscoelastic flow using molecular models: the CONNFFESSIT approach. J. Non-newton. Fluid Mech. **47**, 1–20 (1993)
35. Cueto, E., Laso, M., Chinesta, F.: Meshless stochastic simulation of micro macro kinetic theory models. Int. J. Multiscale Comput. Eng. **9**(1), 1–16 (2011)
36. Roweis, S.T., Saul, L.K.: Nonlinear dimensionality reduction by locally linear embedding. Science **290**(5500), 2323–2326 (2000)